Int. J. Electrochem. Sci., 14 **(2019)** 3070 – 3080, doi: 10.20964/2019.03.43

International Journal of
ELECTROCHEMICAL
SCIENCE
www.electrochemsci.org

First Principle Study of New W_2N Monolayer: a Promising Candidate for Li^+ ion Batteries

Shafiq Ur Rehman[1], Sayed Ali Khan [1], Waqar Uddin[2] , Qudrat Ullah Khan[1], Maryam Kiani[1], Ikhtisham Mehmood[1], Muhammad Sohail [3] , Muhammad Saeed[3] , Sachin Kumar[1], Ling Zhu[1]*

[1] Shenzhen Key Laboratory of Flexible Memory Materials and Devices, College of Electronic Science and Technology, Shenzhen University, Nanhai Ave. 3688, Shenzhen, Guangdong 518060, P. R. China
[2] School of Chemistry and Chemical Engineering, Anhui University, Hefei 230601, China
[3]I nstitute for advanced study, Shenzhen University, Shenzhen, Guangdong 518060, P. R. China
[*]E-mail: zhuling@szu.edu.cn

Received: 27 July 2017 / *Accepted:* 23 January 2019 / *Published:* 7 February 2019

We have predicted new anode material W_2N monolayer for the application of Li^+ ion batteries by using first principles calculation. The W_2N monolayer is found to be stable energetically and dynamically as well. It is also found that W_2N monolayer is metallic in both IT phase and in 2H phase. Furthermore, the calculated open circuit voltage for the Li^+ adsorbed W_2N monolayer is 0.88V which is suitable voltage for a commercial anode material. The calculated diffusion barrier for the Li^+ ions on the surface of W_2N monolayer is 0.22eV. Due to low diffusion barrier the ions will easily flow over the surface of W_2N monolayer. This will boost the electronic conductivity which is the requirement of an efficient Li^+ ion battery.

Keywords: W_2N monolayer, electronic structure, Li^+ ion battery, adsorption and binding energy, storage capacity, open circuit voltage.

1. INTRODUCTION

Lithium ion batteries (LIBs) have wide range of application due to high energy storage, reversible capacity, high power density and long life cycle [1-9]. Currently, LIBs have advantages in the electronic and photonic devices such as mobile phones, laptop, computer, electric vehicles, and optoelectronic devices as well [10-13]. The efficiency of LIBs is highly dependent on the performance of their electrode materials. Therefore, many efforts have been made to find appropriate materials which can enhance the performance of the Li^+ ion and Na^+ ion batteries [14,5,15]. Furthermore, researchers have been successfully investigated some proper anode materials for the better performance of metal ion batteries

[6,16-18]. The most widely used 2D material graphene have played an important role to improve the electrochemical performance of the LIBs. The excellent electrical and chemical properties and low cost of graphene make it a potential candidate for the applications in LIBs [4,1]. Many more 2D materials like, silicene, transition metal dichalcogenides and MX-enes have also shown better electrochemical performance and hence successfully used as anode materials in LIBs [7-10,13,6].These two dimensional semiconductor monolayer materials are best consider for the rechargeable batteries as an anode. For example the transition metal carbides (Mo_2C and W_2C) monolayers have metallic nature, high mechanical strength, thermal and dynamical stability and high charge capacity, such characteristics make transition metal carbides a promising candidate for application to the LIBs [19,5]. Similarly, the other 2D monolayers MoS_2, $MoSe_2$, TiS_2 and SnS_2 have been synthesized both experimentally and theoretically. The electrodes based on these 2D monolayers have been successfully employed in LIBs [20,11,21-24]. It is found experimentally, that MoS_2 has a high storage capacity and is consider a promising anode material for the LIBs [25,26]. First principle calculations have shown that MoS_2 monolayer have high adsorption energy and low diffusion energy barrier [27]. But MoS_2 monolayer is a semiconductor material with direct energy gap 1.8eV, which cause a failure to good electrical conductivity in the MoS_2 monolayer and hence, limits its electrochemical performance. Therefore, an alternate ideal candidate (anode material) is required to circumvent this barrier. Density functional theory (DFT) can be used to predict new efficient anode materials, for example VS_2, MoS_2, W_2C and TiS_2 monolayers has been investigated using DFT, which have high adsorption capability to the Li^+ ion and also have high Li^+ ion storage capacity [28-30]. Similarly, other low dimensional materials have been predicted theoretically and later successfully prepared in experiment and their electronic, electrical and optical properties have been studied [31-34]. Very recently, W_2C monolayer has been predicted using first principle calculation and is expected to achieve in experiment [30]. Therefore, in this study we employed the same theoretical approach (DFT) and predict a new monolayer W_2N with metallic character having open circuit voltage 0.8V. This value of open circuit voltage is very near to the calculated open circuit voltage of MoS_2, VS_2 and W_2C monolayer predicted by density functional theory calculation [28-30]. Similar to the reported (Mo_2 N,W_2C) monolayers we also predict, that W_2N monolayer exist in to two phases called 2H phase and 1T phase [34]. In 2H phase the N atom is sandwiched between two W atoms with AB stacking while in 1T phase the N atom is sandwiched between two W atoms with ABC stacking. The 1T (ABC stacking) and 2H (AB stacking) monolayer structures of W_2N are shown on left side of Figure.1 respectively. Since, in this paper we actually present (W_2N monolayer) an analogue to the previously predicted monolayers, with high electronic mobility, high specific capacity and high kinetic stability, which are the requirements of an efficient battery.

2. METHODOLOGY

We used density functional based code VASP with the generalized gradient approximation (GGA) suggested by Perdew, Burke and Ernzerhof [35-36]. The 1T and 2H structures of W_2N monolayer were optimized with cutoff energy 360 eV, 5×5×1 K-point for the optimization were considered. 1T and 2H structures of W_2N monolayer were fully optimized until the allowed error in the

total energy is less than 10^{-4} eV and the error in the forces is smaller than 2×10^{-2} eV/Å. Phonon calculation was performed with the phonopy code to find the dynamic stability of W_2N monolayer. The nudge elastic Model (NEB) were used to study the minimum energy path for the flow of Li^+ ion from one T2-site to another T2-site on the surface of W_2N monolayer and to estimate the Li^+ ion diffusion barrier [37].

3. RESULT AND DISCUSSION

We first built the bulk structures of W_2N in two different phases i.e 2H-phase and 1T phase and then convert each structure in to pristine monolayers as shown on the left side of Figure.1.These monolayers were relaxed and their structure parameters were studied. The relaxed lattice parameters for 2H phase of W_2N monolayer is (a=b= 2.84Å) and the bond length W-N is (2.16Å) and for 1T monolayer lattice parameters (a=b= 2.89Å), bond length (W-N=2.12Å) which were in agreement with the reported work [30].

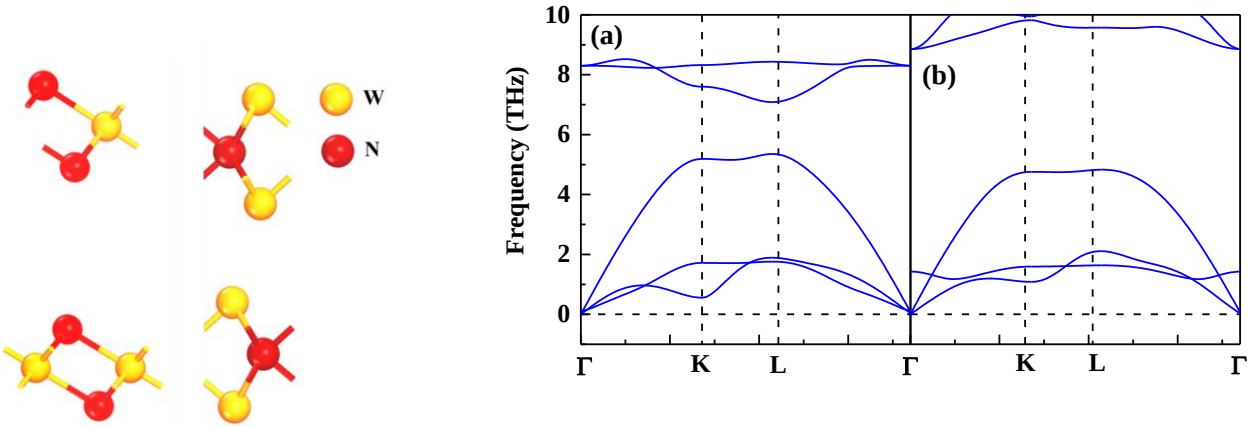

Figure 1. Left side, 1T and 2H structures of W_2N monolayer respectively. Right side, the calculated phonon band structures for the dynamical stability of W_2N monolayer a) for 1T-phase b) for 2H-phase.

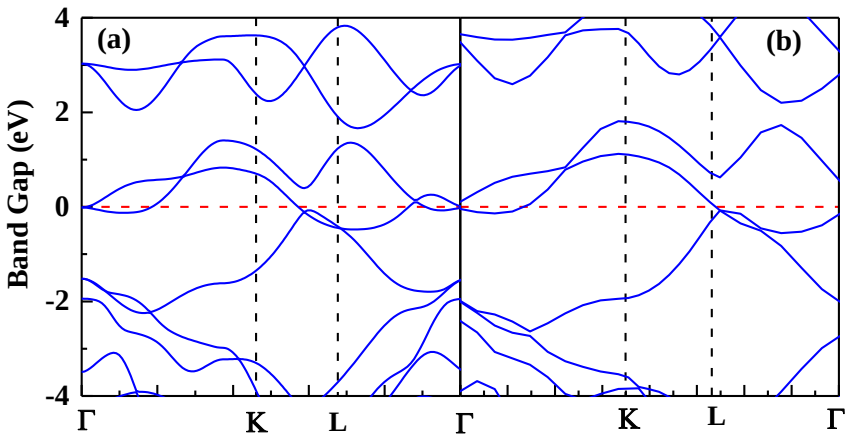

Figure 2. Electronic band structures of W_2N monolayer a) for 1T-phase b) for 2H-phase. W_2N monolayer is found to be metallic both in 2H-phase and in 1T-phase.

The energetic stability were found with the formation energy formula $Ef = (E_{W2N} - 2E_W - E_N)/3$. Where E_{W2N} is the energy of a single W_2N layer per unit cell, E_W and E_N are the energies of W and N atoms respectively per unit cell. The calculated formation energy for W_2N in 2H phase is -8.25 and in 1T phase is -8.47. The negative formation energy shows that both phases of W_2N are stable. Further the dynamical stability of 2H and 1T phase of W_2N were checked with the phonon calculation. The phonon calculation on the right side of Figure.1 shows that both phases are stable dynamically. Because all frequencies are greater than zero and no imaginary frequencies are found. Furthermore, the electronic structures of W_2N monolayer were studied in the term of band structure shown in Figure.2. It is found that W_2N monolayer is conductor in both phases 2H and 1T. Because no band gap were found in the band structure and there is an overlapping behavior at the Fermi level.

3.1 Adsorption and Diffusion

Adsorption and diffusion are two important processes through which we can study the suitability of a material for the synthesis of electrodes. Because adsorption of ions on the surface of electrode material gives us the charge storage capacity of the electrode material and diffusion is related to the electronic mobility and charge/discharge rate of the electrode material, the selection of the proper electrode material for a battery based on these terminologies.

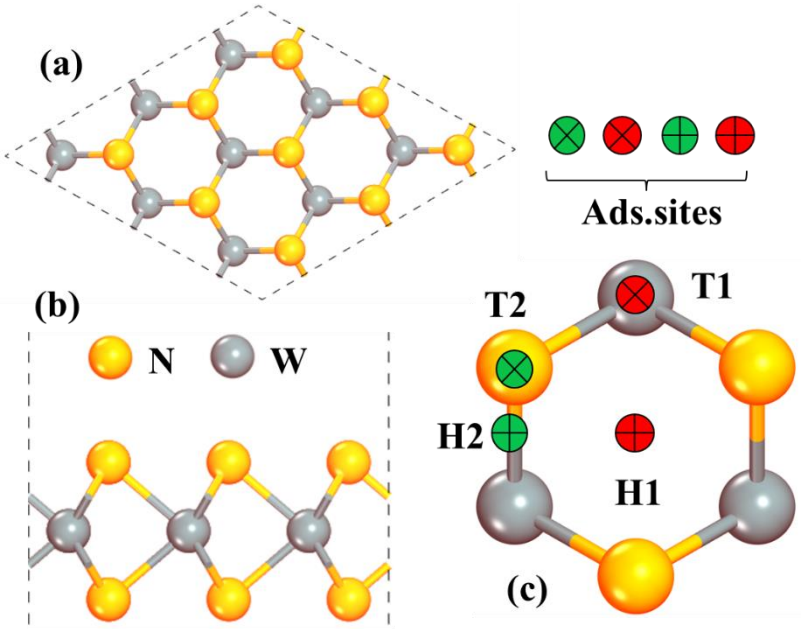

Figure 3. The ball and stick models of W_2N monolayer with 3×3×1 super cell after relaxation a) top side b) across view c) considered adsorption positions on W_2N monolayer.

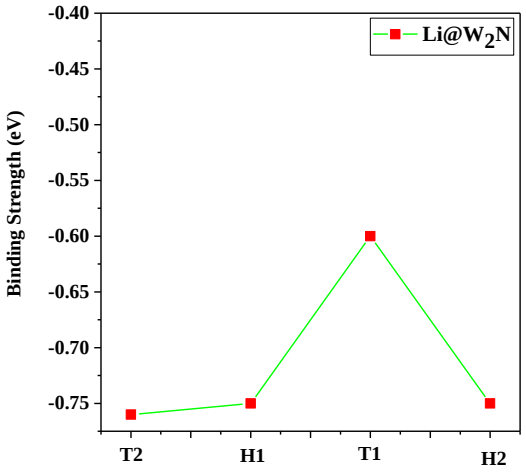

Figure 4. Adsorption energy as a function of Li^+ion adsorption on a single W_2N layer where T2, H1, T1 and H2 are adsorption site.

Therefore it is necessary to study the adsorption and diffusion of the Li^+ ion on the surface of the W_2N monolayer to confirm eighter W_2N monolayer is a desirable electrode material for Li^+ ion batteries. But for the adsorption of Li^+ on the surface of W_2N monolayer favorable adsorption sites are required, which is the site of minimum adsorption energy of Li^+ ion on the W_2N monolayer. Therefore we defined the adsorption energy $E_{Ad} = E_{LiW_2N} - E_{W_2N} - E_{Li_{bulk}}$, where E_{LiW_2N} is the total energy of Li^+ ion adsorbed W_2N monolayer, E_{W_2N} is the energy of isolated W_2N monolayer and $E_{Li_{bulk}}$ is the total energy for the bulk Li^+. Now we employ this formula to the W_2N single layer to find the most favorable position for the Li^+ ion adsorption on the W_2N monolayer and then will consider the similar minimum energy position for the adsorption of all Li^+ ions on the W_2N nanosheet with 3×3×1 super cell. According to the geometry of the W_2N monolayer we consider four possible positions for the adsorption of Li^+ ion i.e the exact top positions on W and N are T1and T2 respectively as shown in Figure.3.

While H1 is the center of the hexagon and H2 is the center of the W-N bond length. The calculated adsorption energy for Li^+ adsorption on each position is shown in Figure.4. Where the most favorable position for the Li^+ adsorption is T2 i.e exact the top position of N. Because the ground state energy is at T2 position. The minimum adsorption energy of the Li^+ ion at the T2 site is -0.77eV with a distance from T2 is 2.5 Å. Further, to see the effect of Li^+ ion adsorption on the absolute binding energy in the 3×3×1 super cell we have calculate the absolute binding energies as a function of Li^+ ion concentration *x* adsorbed on the surface of W_2N monolayer with 3×3×1 super cell. Figure.5 shows the ball and stick model of Li^+ adsorbed W_2N monolayer (Li^+@W_2N monolayer). Figure.5 (a) shows the top view of Li^+@W_2N monolayer and Figure.5 (b) is the side view of Li^+@W_2N monolayer. Where the pink ball represents the Li^+ ion adsorbed on the surface of W_2N monolayer. There are total nine available sites for the Li^+ ion adsorption as shown in Figure.5 (b). Since we can adsorb maximum of nine Li^+ ions on the surface of W_2N monolayer with 3×3×1 super cell. Therefore we choose Li^+ ion concentration; x=*0.1–0.9.*

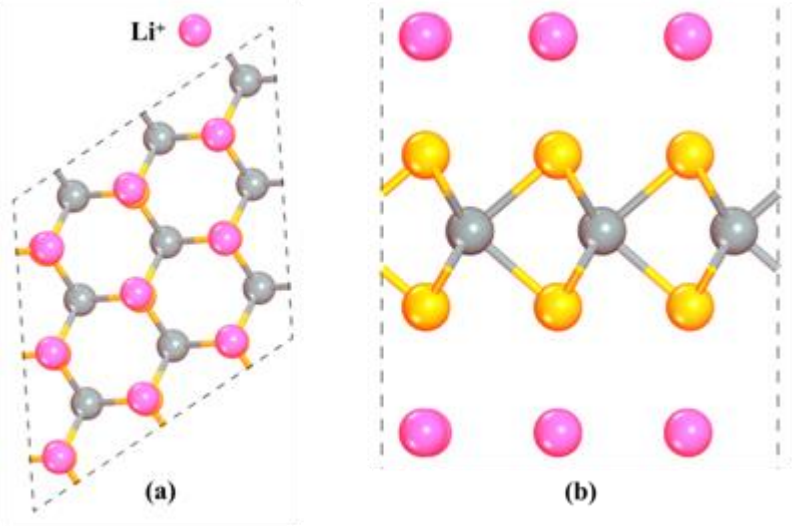

Figure 5. The ball and stick models of Li^+@W_2N monolayer with 3×3×1 super cell after relaxation a) top side b) across view. Where the pink balls represents Li^+.

The absolute binding energy of Li^+ ions adsorption on the surface of W_2N sheet is given as $E_b = (E_{W_2N} - E_{W_2N+Li} + xE_{Li_{bulk}})/x$. Where E_{W2N} is the total energy of the relax W_2N single layer and $E_{W_2N} + Li$ is the energy of Li^+ adsorbed W_2N monolayer system, $E_{Li_{bulk}}$ is the energy of Li^+ in its bulk crystal form and x is the number of Li^+ ions. The calculated binding energy according to this formula is plotted in Figure.6. The higher binding energies of the Li^+ adsorption on W_2N monolayer means that Li^+ ion transfer their charge to W_2N and make strong bonds with the surface of W_2N monolayer and also shows high storage capacity of the W_2N monolayer to Li^+ ions. Furthermore, the dependencies of Li^+ ions on the binding energies have been studied; the binding energy shows a linear decrease with Li^+ ion concentrations. This is because every Li^+ ion adsorbed on the surface of W_2N monolayer give electrons to the W_2N monolayer and gets positively charged so with the increasing Li^+ ions the Li^+-Li^+ distance will be decrease and the coulomb electrostatic force between Li^+ and N will be overcome by the strong repulsive force between Li^+–Li^+ ions. This will make apart the Li^+ ions from the surface of the W_2N and result will be decrease in the binding energy. Hence the two factors the distance between the ions and the decrease in the net charge on the Li^+ ions affects the binding energy. But still the binding energies are higher than zero so the adsorption of Li^+ ions will not form a metal cluster. Second the higher binding energies for the Li^+ ions means that the W_2N monolayer has strong capacity to the Li^+ ions adsorption. So the W_2N monolayer plays an important role in the Li^+ ions batteries.

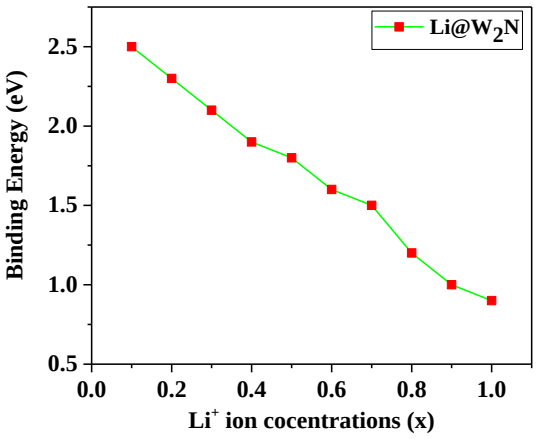

Figure 6. Binding energy graph for the Li^+ adsorption on W_2N sheet as a function of Li^+ ion concentration; *x=0.1–0.9*

3.2 Open Circuit Voltage

The efficiency of a battery depends on the open circuit voltage (OCV); if the battery has low OCV it will be more reliable. Thus the electrode materials having low open circuit voltage are best consider for the application to the battery. Therefore we theoretically estimate the OCV by the reported equation $\varepsilon_{OCV} = -(V_{LiW_2N} - V_{W_2N} - xV_{Li_{bulk}})/xe$. Where ε_{OCV} is the open circuit voltage, V_{W_2N} is the total energy of the W_2N monolayer sheet consider for calculation , V_{LiW2N} is the total energy of the W_2N monolayer nanosheet plus adsorbed Li^+ ion and the last term is the total energy in the bulk crystal structure of the Li^+. Open circuit voltage has been estimated by this formula for all the Li^+ ion concentration adsorbed at T2 position on the W_2N monolayer sheet as shown in Figure.7. The height of the red column defines the value of the OCV. The highest amount of OCV when all the T2-site are filled with Li^+ ions is 0.88V and the lowest is 0.33 V. The OCV values reported for VS_2, Mo_2C, W_2C and SnS_2 are 0.92V, 0.84V and 1V respectively [5, 11-12, 19-20]. The reported OCV for TiS2 monolayer with maximum Li^+ ions adsorbed at the TiS2 surface is 1.29V this value of OCV is too high thus TiS_2 is not suitable for the Li^+ ion battery, because it is also reported that OCV should be lower than 0.8V for the commercial application and should be greater than zero to avoid the dendrite formation [12]. While calculated OCV in the same TiS_2 monolayer for the maximum Na^+ ion adsorption is 0.92V, therefore TiS_2 monolayer is consider a good candidate for the Na^+ ion battery while less efficient for the Li^+ ion battery. It is also reported that MoS_2 could be used as the anode material for Na ion batteries, which has a maximum theoretical specific capacity 146 mAh·g−1, open circuit voltage range 0.75−1.25 V and diffusion barrier 0.68 eV [38-39]. A similar study is also carried out on MoN_2 monolayer, a high specific capacity 864 mAh·g−1 and low open circuit voltage (0.62 V) has been achieved [40]. The layered materials (Na2Ti3O7) have also been studied as a potential anode material for NIBs [41]. Through optimization of the electrolyte and binder, the reversible capacity of Na2Ti3O7 is found to be 188 mAh·g−1 and the average Na storage voltage is found 0.3V. While In our calculation the voltage range 0.88V-0.33V and the maximum specific capacity is 290 mAh/g when all the nine available sites are filled with Li^+ ions, since W_2N monolayer is quite suitable to use it as an anode material commercially.

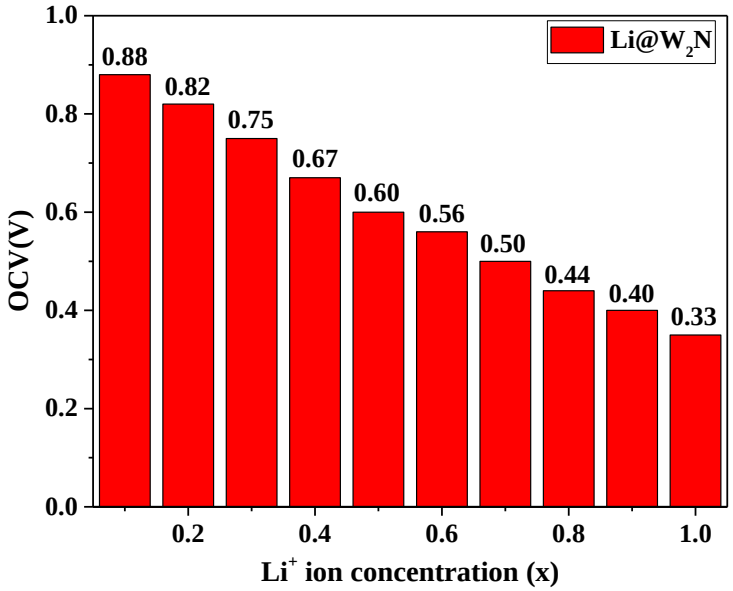

Figure 7. Column graph representation of OCV Vs. Li^+ ion concentration where the voltage rang is 0.88– 0.33V.

3.3 Specific Capacity

The amount of ions stored by a battery is term as specific capacity. The specific capacity of an electrode material can be defined as $\chi = xF / N_{W_2N}(mAh\,g^{-1})$. Where χ is the specific capacity with SI unit $(mAh\,g^{-1})$, x is the number of ions adsorbed on the surface of W_2N monolayer sheet and F is faraday constant (26801mAh/mol) and N_{W_2N} is the molar mass of W_2N nanosheet. The calculated value of the specific capacity is 290 mAh/g for Li^+ ions. This value of specific capacity is quite better than MoS_2 and other layered materials [38-39]. The flow of Li^+ ions in the battery between the cathode and anode can be written in the form of a chemical reaction as $xLi^+ + xe^- + W_2N \Leftrightarrow Li_xW_2N$. The negative ions generated during this reaction flow in the outer part of the battery while the positive ions move inside the battery between the two electrodes. To create more and fast ions in the battery, electrode material of high electrical conductivity are required. Thus W_2N can be used as an electrode material in this situation because of its metallic nature and higher charge mobility as we discussed above. Further to see the effects of ions on the electronic structure of W_2N monolayer we have investigate its electronic structures in the term of projected density of states (PDOS) as shown in Figure.8. The PDOS shows that when we increase the Li^+ ions concentration the intensity of the peak at the Fermi level is increases which shows the W_2N monolayer become more and more conductive and hence the electrical conductivity of W_2N monolayer increase. Previously investigated anode materials like graphene and MoS_2 which are insulator and semiconductor respectively, have intrinsically very low conductivity. Although some strategies like doping can be used to make these materials metallic but this will increase the diffusion barrier and will make them most costly electrode material.

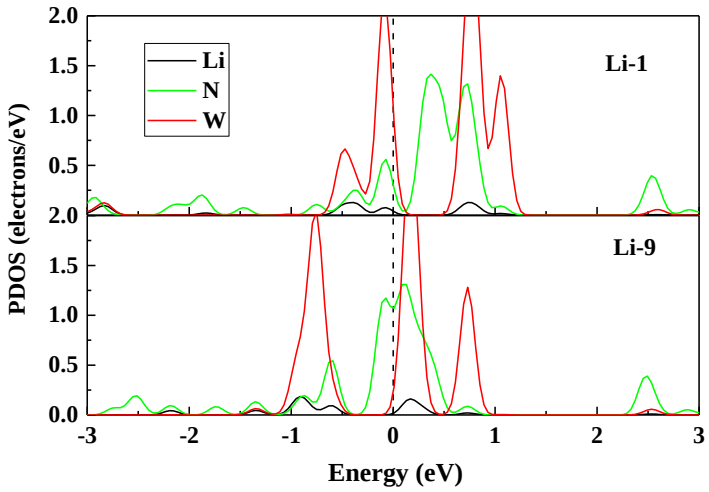

Figure 8. Projected Density of states (PDOS) for a) Li^+ =1 and b) Li^+ =9. The PDOS shows the metallic behavior of W_2N during Li^+ ions adsorption.

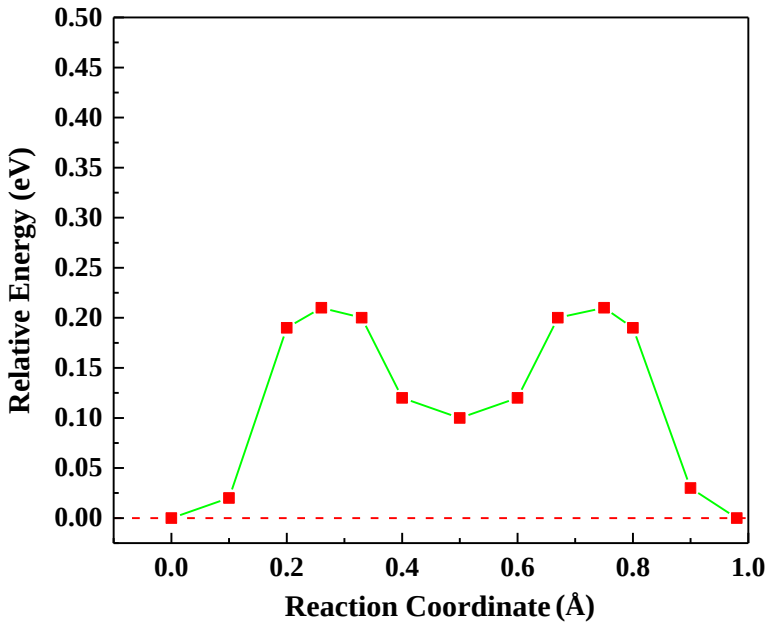

Figure 9. Li^+ ions minimum energy path from T2 site to near by T2-site through H-site on the surface of W_2N nanosheet with calculated diffusion barrier is 0.22 eV.

One of the most important property of an electrode material is the easy flow of ions inside the anode material because the fast and easy flow of ions will give the high mobility, which will increase the performance of the battery. Therefore we define the term diffusion and diffusion barrier, the diffusion at the surface of the monolayer occurs when a Li^+ ion move from one position to another. Obviously the minimum energy path is from one T2-site to another T2-site while passing through H-site. This gives a barrier of 0.22eV in good agreement with reported work even better than the MoS_2 monolayer [19-20, 42].

4. CONCLUSION

In summery we have performed density functional theory calculations and predict W_2N monolayer for the application to the Li^+ ion batteries. The W_2N monolayer is found to be stable energetically and dynamically as well. It is also found that W_2N monolayer is metallic in both IT phase and in 2H phase. Furthermore, the calculated open circuit voltage range for the Li^+ adsorbed W_2N monolayer is 0.88-0.33V which is suitable voltage rang for a commercial anode material. The calculated diffusion barrier for the Li^+ ions on the surface of W_2N monolayer was found 0.22eV. Due to this low diffusion barrier the ions will easily flow over the surface of W_2N monolayer. This will boost the electronic conductivity which is the requirement of an efficient Li^+ ion battery.

ACKNOWLEDGEMENT
This work was financially supported by the grants from the Science and Technology Innovation Commission of Shenzhen (Grant No. ZDSYS201707271554071.

References

1. Y. Shi, L. Wen, G. Zhou, J. Chen, S. Pei, K. Huang, H.-M. Cheng, F. Li, *2D Materials*, 2 (2015) 1-024004.
2. N.K. Jena, R.B. Araujo, V. Shukla, R. Ahuja, *ACS Appl. Mater. Interfaces*, 9 (2017) 16148-16158.
3. L. Shi, A. Xu, T. Zhao, *ACS Appl. Mater. Interfaces*, 9 (2017) 1987-1994.
4. D. Er, E. Detsi, H. Kumar, V.B. Shenoy, *ACS Energy Lett.*, 1 (2016) 638-645.
5. Q. Sun, Y. Dai, Y. Ma, T. Jing, W. Wei, B. Huang, *J. Phys. Chem. Lett.*,7 (2016) 937-943.
6. G.-C. Guo, D. Wang, X.-L. Wei, Q. Zhang, H. Liu, W.-M. Lau, L.-M. Liu, *J. Phys. Chem. Lett.*,6 (2015) 5002-5008.
7. Y. Xie, Y. Dall'Agnese, M. Naguib, Y. Gogotsi, M.W. Barsoum, H.L. Zhuang, P.R. Kent, *ACS Nano*,8 (2014) 9606-9615.
8. X. Tan, C.R. Cabrera, Z. Chen, *J. Phys. Chem. C*, 118 (2014) 25836-25843.
9. C. Chowdhury, S. Karmakar, A. Datta, *ACS Energy Lett.*, 1 (2016) 253-259.
10. D. Dubal, O. Ayyad, V. Ruiz, P. Gomez-Romero, *Chem. Soc. Rev.*,44 (2015) 1777-1790.
11. Y. Xiao, J.-Y. Hwang, Y.-K. Sun, *J. Mater. Chem. A*, 4 (2016) 10379-10393.
12. H. Zhang, M. Zhang, M. Zhang, L. Zhang, A. Zhang, Y. Zhou, P. Wu, Y. Tang, *Journal of Colloid and Interface Science*, 501 (2017) 267-272.
13. Q. Peng, X. Sun, H. Wang, Y. Yang, X. Wen, C. Huang, S. Liu, S. De, *Appl. Mater. Today*, 7 (2017) 169-178.
14. D. Er, E. Detsi, H. Kumar, V.B. Shenoy, *ACS Energy Lett.*, 1 (2016) 638-645.
15. Y. Xiao, J.-Y. Hwang, Y.-K. Sun, *J. Mater. Chem. A*, 4 (2016) 10379-10393.
16. H. Zhang, M. Zhang, M. Zhang, L. Zhang, A. Zhang, Y. Zhou, P. Wu, Y. Tang, *Journal of Colloid and Interface Science*, 501 (2017) 267-272.
17. M. Moura, R. Barrada, J. Almeida, T. Moreira, M. Schettino, J. Freitas, S. Ferreira, M. Lelis, M. Freitas, *Chemosphere*, 182 (2017) 339-347.
18. J. Li, S. Xiong, Y. Liu, Z. Ju, Y. Qian, *ACS Appl. Mater. Interfaces*, 5 (2013) 981-988.
19. Y. Huang, C. Ling, X. Chen, D. Zhou, S. Wang, *RSC Advances*, 5 (2015) 32505-32510.
20. Y. Jing, Z. Zhou, C.R. Cabrera, Z. Chen, *J. Phys. Chem. C*, 117 (2013) 25409-25413.
21. Y. Huang, C. Ling, X. Chen, D. Zhou, S. Wang, *RSC Advances*, 5 (2015) 32505-32510.
22. D. Wang, L.-M. Liu, S.-J. Zhao, Z.-Y. Hu, H. Liu, *J. Phys. Chem. C*, 120 (2016) 4779-4788.

23. F. Ersan, G.k. Gökoğlu, E. Aktürk, *J. Phys. Chem. C*, 119 (2015) 28648-28653.
24. L. Jiang, B. Lin, X. Li, X. Song, H. Xia, L. Li, H. Zeng, *ACS Appl. Mater. Interfaces*, 8 (2016) 2680-2687.
25. G. Du, Z. Guo, S. Wang, R. Zeng, Z. Chen, H. Liu, *Chem. Commun.*, 46 (2010) 1106-1108.
26. H. Hwang, H. Kim, J. Cho, *Nano lett*., 11 (2011) 4826-4830.
27. Y. Li, D. Wu, Z. Zhou, C.R. Cabrera, Z. Chen, *J. Phys. Chem.* Lett., 3 (2012) 2221-2227.
28. D. B. Putungan, S-H. Lin, J-L. Kuo *ACS Appl. Mater. Interfaces*,8 (2016)18754-18762.
29. E. Yang, H. Ji, and Y. Jung, *J. Phys. Chem. C*, 119 (2015), 26374.
30. J. Li, S. Xiong, Y. Liu, Z. Ju, Y. Qian, *ACS Appl. Mater. Interfaces*, 5 (2013) 981-988.
31. H. Zheng, X-B. Li, N-K. Chen, S-Y. Xie, WQ. Tian, Y. Chen, H. Xia, S. Zhang, H-B. Sun, *Phys. Rev. B* 92 (2015) 115307.
32. L. Guan, G. Chen, J. Tao, *Phys.Chem. Chem. Phys*., 18(2016) 15177-1518.
33. C. Bacaksiz, R. Senger, H. Sahin, *Appl Surf. Sci*., 409(2017)426-430.
34. M. Safari, Z. Izadi, J. Jalilian, I. Ahmad, S. Jalali-Asadabadi, *Phys. Lett. A*, 381(2017) 663-670
35. X. Zhang, Z. Yu, S-S. Wang, S. Guan, H.Y. Yang, Y. Yao, S.A. Yang, *J. Mater. Chem. A*, 4 (2016) 15224-15231.
36. G. Kresse and J. Furthmüller, *Phys. Rev. B*, 54 (1996) 11169.
37.P. Perdew, K. Burke and M. Ernzerhof, *Phys. Rev. Lett.*, 77 (1996) 3865.
38. D. Sheppard, R. Terrell and G. Henkelman, *J. Chem. Phys.*, 128 (2008) 134106.
39. M. Mortazavi, C. Wang, J. K. Deng, V. B. Shenoy, N.V. Medhekar, *J. Power Sources*, 268 (2014), 279−286.
40. L. David, R. Bhandavat, G. Singh, G. *ACS Nano*, 8 (2014) 1759−1770.
41. Z. Lan, M. Chen, X. Xu, Xiao, F. Wang, Y. Wang, Y. Lu, Y. Jiang, J. Jiang, *J. Alloys and Compounds*, 701 (2017) 875-881.
42. H. L. Pan, X. Lu, X. Q.Yu, Y. S. Hu, H. Li, X. Q.Yang, L. Q. Chen, *Adv. Energy. Mater*, 3(2013) 1186−1195.
43. H. J. Chen, J. Huang, X. L. Lei, M. S. Wu, G. Liu, C. Y. Ouyang, B. Xu, *Int. J. Electrochem. Sci.*, 8 (2013) 2196 – 2203.

© 2019 The Authors. Published by ESG (www.electrochemsci.org). This article is an open access article distributed under the terms and conditions of the Creative Commons Attribution license (http://creativecommons.org/licenses/by/4.0/).